Soft Matter

Accepted Manuscript

ROYAL SOCIETY OF CHEMISTRY

www.rsc.org/softmatter

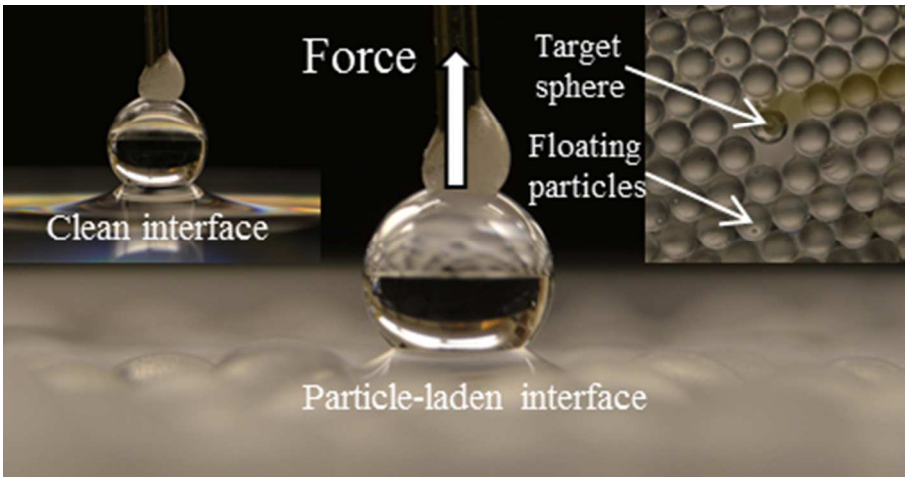

Measured Capillary Forces on Spheres at Particle-Laden Interfaces

Wei He, Nesrin Şenbil, A. D. Dinsmore

ABSTRACT

We measure capillary forces on particles at fluid interfaces in order to assess the key parameters that yield effective stabilizing particles. In our experiments, a millimeter-scale particle is attached to a cantilever, which is used to pull the particle perpendicular to the interface. Simultaneously, we image from the side to measure the cantilever's deflection and thus the pulling force, as well as the height of the particle and the shape of the interface. We find that the peak force on a particle at an interface crowded with other particles is consistently smaller than the force at a clean interface. This result is independent of the difference in fluid mass densities, the material of the target sphere, and the capillary charge of the free particles. We attribute the force reduction to the perturbation of interface shape due to the constraints at the boundaries of the free particles. The results should be helpful in designing particles to stabilize droplets in new oil dispersants or in other applications.

Introduction

With the potential for particles to stabilize droplets established a century ago, surfactant-free particle-stabilized (Pickering) emulsions are now widely used in many fields such as biomedical, food products and oil-spill cleanup [1-8]. In the formation of a Pickering emulsion, solid particles absorb onto the interface between the two phases and therefore prevent the coalescence of droplets. Emulsion stability largely depends on the behavior of those particles bound at interfaces. This makes it important to understand the fundamental physics of the capillary interaction on particle-laden interfaces. The understanding of the adsorption and desorption of particles at fluid interfaces paves the way to the design of optimal particulate dispersants that could efficiently stabilize emulsions. Early progress on this problem came from a geometric model, by Koretsky and Kruglyakov [2] and Pieranksi [3], of the binding energy for individual spheres at a clean, planar interface assuming that the contact angle is given by the equilibrium Young-Dupré value. Later work showed how the adsorption can be controlled by the fluid interfacial tension and by properties of the individual particles such as shape, roughness, and surface chemistry [9-14]. Pitois and co-workers [15] showed that hysteresis in the contact angle leads to a different force for inserting and withdrawing a sphere at an interface. They also pointed out that the stability of Pickering emulsions should depend on the work to remove a bound particle (the work of detachment) rather than the equilibrium binding energy. The preceding studies, however, leave out the fact that particle-stabilized droplets may be packed with many particles, leaving open the question of whether the binding energy or work of detachment depends on the presence of other particles at an interface.

In experiments, tensiometry is the classical technique to measure the capillary force, in which small solid bodies are pulled through a fluid interface vertically. The most

commonly used bodies are the (du Nouy) ring, the (Wilhelmy) plate and the sphere [16-21]. After the invention of the atomic force microscope, the behavior of microscopic colloidal particles at interfaces was investigated by attaching the particle to the probe. In this way, capillary forces were measured and contact angles extracted from these data [22,23]. This approach has been used to measure how particle shape and surface roughness affect capillary forces [13,14], which in turn affects emulsion stability [11]. More recently, forces were measured at the same time that interface shape and contact angle were obtained directly from the experiment [15]. This method will be essential for progress on the remaining questions about the role of interface shape and many-particle interactions.

In this paper, we report measurements of the force on a sphere as it is withdrawn from or inserted into an interface between two immiscible fluids. For the case of individual spheres at an initially planar interface, we find results that agree quantitatively with theory and we verify that the receding contact angle is constant during the withdrawal process. When freely floating particles are added to the interface, however, we find that the force-displacement curve changes. In particular the peak force needed to extract the sphere decreases by as much as 39%. We repeat the measurements under various conditions of the mass density of the fluids and of the particle; these results show that the peak-force reduction arises not from gravity or buoyancy, but rather from the capillary force itself. We conclude that fluid-interface-contact conditions around the free-floating particles alter the shape of the interface and thereby reduce the capillary force acting on the target sphere and the work needed to detach it from the interface. We discuss how these results should apply for particles that are micron- or nanometer-sized.

Experimental Section

Materials and Apparatus

Figure 1 shows the schematic of the experimental setup used to insert or withdraw a sphere while measuring the force and imaging the interface shape. In most experiments reported here, we measured the force acting on clean glass spheres coated with polydimethylsiloxane (PDMS) to provide a smooth contact line and consistent contact angle. Borosilicate glass spheres (1/8" diam., manufactured by Winsted Precision Ball Company and purchased from McMaster-Carr, cat. no. 8996K22) were treated using the following procedure: glass spheres were first cleaned by soaking in a sulfuric acid and NoChromix® solution for 12 h and then immersed in deionized water for 6 h (water was changed every 30 min). Once dried, the spheres were functionalized by immersing them in polydimethylsiloxane using 20-mL disposable scintillation vials, baking in an oven for 24 h at 150 °C, then rinsing in toluene (1 h), acetone (1 h) and deionized water (2 h) [24]. After that, the sphere was attached by epoxy (ITW Devcon, no. 14277) to a thin fiber, which was linked to a force-measuring cantilever. We found that capillary tubing (Polymicro Technologies, cat. no. TSP020375) works well as the cantilever. Its stiffness (0.504 ± 0.001 N/m) was obtained by calibration measurements, in which sections of metal wire of known weight were placed at the end of the cantilever and the deflection was measured. The displacement was found to be linear with weight in the range of 0 to 0.28 g (8 data points were used in analysis).

We used polymer spheres as the free-floating particles or, in some cases, as the target sphere (*i.e.*, the one attached to the cantilever). These particles were all purchased from McMaster-Carr: acrylic (R = 1/16" radius, cat. no. 1383K42), high-impact polystyrene (1/16" and 5/64" radius, cat. no. 9374K21 and 9374K23), PTFE (3/64" and 1/16" radius, cat. no, 9660K12 and 9660K13), and chemical-resistant polypropylene (1/16" radius, cat. no. 1974K2). In some experiments, we used pieces of glass coverslips (#1½, 22 mm square, VWR cat. no. 48366-227) as floating particles. All particles were cleaned before each set of experiments by sonicating in methanol, rinsing in deionized water, and then drying in air.

The floating particles are characterized by the capillary force acting on them, referred to as the "capillary charge" by analogy to electrostatics [25-27]: $Q = 2\pi\gamma\sin(\alpha)$, where R_c is the radius of contact ring, γ is the interfacial tension and α is the inclination angle (Fig 1). For particles forming a downward meniscus at interface, Q is defined as positive.

The liquids used in the experiments were deionized water (Milli-Q plus) with a tabulated surface tension of 72 mN/m, two different types of silicone oil with density of 0.96 g/mL and 1.05 g/mL respectively (from Sigma-Aldrich, cat. no. 146153 and 175633) and squalane with density of 0.81 g/mL (Sigma-Aldrich, cat. no. 234311). The experiments were performed at room temperature. Fluids were held in a glass crystallizing dish (KIMAX, cat. no. 23000; used for water-squalane experiments), a centrifuge tube (VWR cat. No. 82018-052; used for water-silicone oil experiments) or a polystyrene tissue culture dish (BD Biosciences cat. No. 353002; used for water-air experiments). The diameters of these dishes were much larger than the capillary length (which was 2.7mm or less).

To keep the pressure constant, the liquid bath was connected to a large liquid reservoir with diameter 100 mm. Therefore, in a given set of experiments the pressure remains the same for a fixed position of the target sphere.

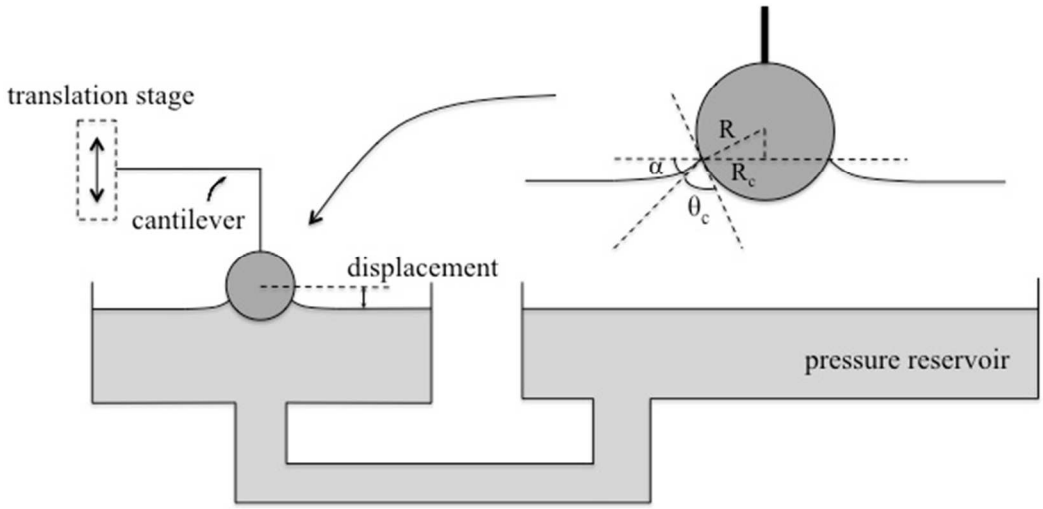

Fig. 1 Schematic of the setup used for force-displacement measurements. Here, R is the sphere radius, R_c is the contact radius, θ_c is the contact angle, and α is the angle between the horizon and the interface at the contact line.

Procedure

In a typical experiment, the height of the target particle was adjusted manually in 0.2-mm increments using the translation stage. After each displacement, the system was allowed to relax for 15 s, after which we saw no additional changes, and then side-view images of the particle region were captured by a digital camera (Nikon D3200 with a Nikon AF-S 18-55 mm lens and 68mm extension tubes) aimed perpendicular to the cantilever.

The force applied by the cantilever was measured from the deflection of the end that is attached to the target sphere. Deflection was measured with a precision of 15 μm by analysis of the images using ImageJ [28]. With this approach, we obtain a typical force resolution of 8 μN. In all cases, we subtracted the weight of the target sphere so that measured $F = 0$ for a sphere in air.

The vertical displacement (d) of the target sphere is defined as the distance between its mass center and the unperturbed interface. When the mass center is above the interface, $d > 0$. Displacement was measured with a precision of 15 μm by image analysis.

To study the effect of free-floating particles, we placed either spheres or pieces of glass coverslips on the interface. The spheres were bound to the interface and formed a two-dimensional hexagonal lattice owing to inter-particle attraction from the Cheerios effect [29,30]. Several particles were removed from the center of the lattice to create a hole that was larger than the target sphere. Hence there was no direct contact between the target sphere and the others throughout the measuring process, so that their effect on the target sphere was only by means of the fluid interface. Likewise, there was no direct contact between the target sphere and pieces of glass coverslips.

Results and Discussion

Force-Displacement Curves

Figure 2 shows the results of a typical experiment, in which we measured $F(d)$ on a PDMS-coated glass sphere at a clean air-water interface (open circles in Fig. 2(b)). Beginning with the particle immersed in water, we raised it in 0.2-mm steps. When the sphere touched the interface, the interface jumped downward to meet the sphere (position 1 on the plot). In this configuration the interface applied an upward force; to balance it the measured force, F, was negative. As the particle was raised further, the contact angle reached a

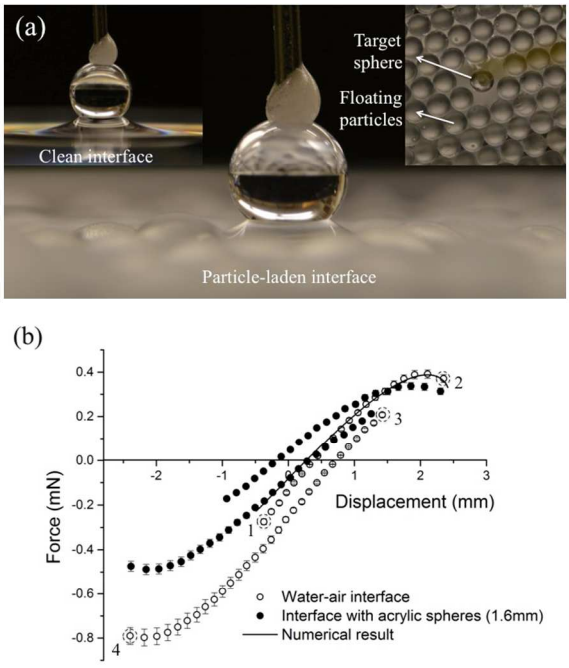

Fig. 2 (a) Side-view and top-view images of a PDMS-coated glass sphere at water-air interface. (***b***) Measured force vs. displacement for the PDMS coated glass sphere at a clean interface (○) compared to the particle-laden interface (●). For each case, the upper (lower) trace shows the results for raising (lowering) the sphere.

steady value. The interface became less deformed and F increased toward zero, then became positive. As the target sphere was withdrawn into the upper air phase ($d > 0$), the interface became more strongly deformed until F reached a peak value. The force then decreased until the fluid bridge ruptured (position 2 on the plot). After this point, the sphere was in air and $F = 0$ (data not shown).

After leaving the sphere in the air phase for several minutes to allow the water on the sphere evaporate, we lowered the target sphere back through the interface. As soon as the sphere touched the interface ($d = R = 1.59$ mm), the interface rose to meet the sphere and applied a downward force (hence $F > 0$; position 3 on the plot). In this case, the fluid interface advanced across the surface of the sphere, so that the advancing contact angle was formed, which was larger than the receding angle. These data are shown by the lower sequence of open circular points in Fig. 2(b). The $F(d)$ curves for pulling out and pushing in were parallel to each other and the gap between them was caused by contact-angle hysteresis [15].

When the positive displacement is large, these data accurately fit the theory of Zhang *et al.* [19] using the measured receding contact angle (90°) and known values of particle size, fluid densities, and interfacial tension. However, near the beginning of the withdrawal process, the measured force was smaller than the theory because the contact angle had not reached its receding value. In the insertion process, the meniscus around the target sphere was below the surface. Such a situation made it difficult to measure the advancing contact angle and thus we did not compare the corresponding force curve with the theory.

We then added free-floating acrylic spheres on the interface and repeated the experiment with the same target sphere. The interface was packed with the spheres of positive capillary charge (Fig. 2(a)) except for the hole around the target sphere. The data show the same general trend as before, but the shape of the $F(d)$ curve was altered and the value of the peak force was significantly reduced both on the air side ($d > 0$) and the water side. In particular, the magnitude of the peak force fell by 14% when raising the sphere and by 39% when lowering it. Both of these changes are repeatable and exceed our measurement uncertainty. In the following discussion, we will focus on the peak force because it is well-defined, easily measured, and independent of error in measuring the displacement (d) of the target sphere. We emphasize that, as in all of our particle-laden-interface experiments, the target sphere is not in contact with the other spheres. Hence the effect on F was by means of the interface itself.

To check the reversibility, we removed the floating acrylic particles from the system and repeated the force measurement, again using the same target sphere. The data (not shown) are indistinguishable from the open circular points. The reversibility was tested several times for all water-air systems, and the results are consistent.

We now turn to experiments using fluids and particles of different mass densities. Figure 3(a) shows measured $F(d)$ curve for a PDMS-coated glass sphere at a water-oil interface. Here, the upper fluid phase is silicone oil ($\rho = 0.96$ g/mL) and the lower fluid phase is deionized water so that $\Delta\rho = 0.04$ g/mL. For clarity, we show only the data for pushing the sphere downward (similar to the lower curves in Fig. 2(b)). As in the case of the water-oil interface, we compare the $F(d)$ curves for an isolated sphere to the curves for a particle-laden interface (with polystyrene spheres of positive capillary charge, R=1.59 mm). The resulting $F(d)$ differs from the water-air experiments because of the

different interfacial tension, contact angle and buoyancy. Nonetheless, we again find that the peak-force value is substantially reduced (here, by 9%) in the presence of the free spheres, despite the fact that the density mismatch of the two fluids was reduced by a factor of 25 compared to the water-air case. In this experiment, the calculated buoyant force acting on the sphere in the water and oil phases, respectively, is 0.164 mN and 0.158 mN, so that any change due to buoyancy could not affect the force by more than 6 μN, which is much smaller than the shift in force that we found.

Figure 3(b) shows the $F(d)$ curve for pushing a PDMS-coated glass sphere (1.59 mm in radius) from air into water containing sodium polytungstate, added to raise the mass density to $\rho = 1.6$ g/mL. The higher mass density of the lower fluid caused the free-floating particles (here, polypropylene) to create upward-sloped menisci at the interface (capillary charge Q is negative). Once again, the interface that is laden with buoyant particles has a substantially lower peak force (by 18%) than the single-particle case for the same fluids.

So far, all target spheres used in experiments were PDMS-coated glass spheres. To extend the results to a more general case, we conducted experiments using different types of target spheres and floating particles. Figure 3(c) shows the measured force on a PTFE sphere (1.59 mm in radius) at a water-silicone oil interface. Here we used silicone

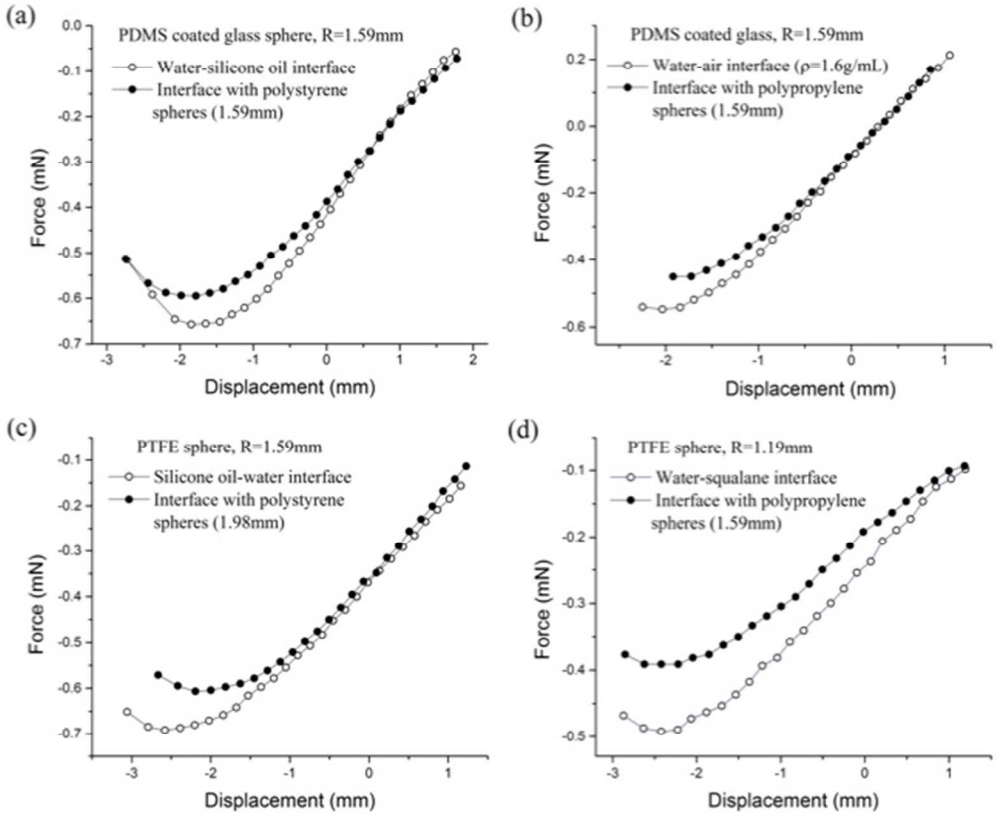

Fig. 3 Measured force vs. displacement for different target spheres at different interfaces, providing examples with free spheres that are negatively buoyant (a), (c), positively buoyant (b), or nearly neutrally buoyant (d) free spheres, and with target spheres that are PDMS-coated glass (a), (b) or PTFE (c), (d). In each case, only the data for lowering the sphere is shown and the clean interface (○) is compared to the particle-laden interface (●).

oil with $\rho = 1.05$ g/mL, floating on water containing sodium polytungstate to achieve $\rho =$ 1.05 g/mL. Hence, $\Delta\rho < 0.01$ g/mL, which is at least 100× smaller than water-air. As floating particles, we use polystyrene, which is also approximately density matched ($\rho =$ 1.05 g/mL) and has slightly positive capillary charge. Once again, we found a substantial reduction of the peak force (by 12%) on the particle-laden interface.

Figure 3(d) shows the measured $F(d)$ on a small PTFE sphere (1.19 mm in radius) at the interface between water and squalane ($\rho = 0.81$ g/mL). Polypropylene spheres were used as floating particles. These particles have a density between that of water and squalane and they are approximately neutrally buoyant; the interface around a single polypropylene bead had no measurable deformation (capillary charge Q is zero). Once again, the details of $F(d)$ differ from the water-air case but the particle-laden interface has a smaller peak force (by 21%).

In all these cases, the data show a systematic reduction of the peak force in the presence of free-floating particles, irrespective of whether the particles deform the interface upward, downward, or not at all; whether the target sphere is a PDMS-coated glass or solid PTFE; and whether the two fluids are of different density or similar density. The results indicate that the force reduction does not arise from gravity acting on the fluids or particles.

This conclusion is not limited to the above-mentioned five cases. As target spheres, we also tested clean (non-functionalized) glass, nylon, polystyrene, polypropylene and acrylic spheres of different sizes. In those experiments, floating objects were nylon, polystyrene, polypropylene, acrylic spheres or small randomly shaped pieces of glass coverslips. All these combinations led to a force reduction.

Distance Scaling

In Fig. 4, we show how the size of the hole in layer of free-floating particles affects the change in the peak force (ΔF_{peak}). In this case, we used a nylon sphere as the target and polypropylene spheres as the free spheres. The peak force was measured for withdrawing the sphere from an air-water interface. The hole size was defined as the shortest distance between the center of the hole and the edge. As expected, when the size of the hole approaches the size of the dish (*i.e.* there is only a double ring of particles far away), these particles have no discernible effect on the target sphere. We fit the data to an exponential curve, $\Delta F_{peak} = C\exp(-a_h/\xi)$, where C and ξ are fit parameters and a_h is the size of the hole. We found a best fit for $C = 0.8$ and $\xi = 2.8$ mm; the latter is close to the calculated capillary length for water-air ($(\gamma/(\Delta\rho\, g))^{1/2} = 2.7$ mm). Hence, it appears that the free-floating particles only affect the peak force when they are close enough to affect the interface shape. This result indicates that the reduced force is mediated by an altered interface shape.

Interface Shape

By what mechanism do the free-floating particles alter the force on the target sphere? To address this question, we first point out that the measured force applied by the cantilever must balance a sum of five forces acting on the target sphere: (*i*) the capillary force, which comes from the fluid-fluid interface pulling around the ring of contact; (*ii*) the Laplace pressure acting on the surface of the target sphere that is exposed to the lower fluid; (*iii*) buoyancy of the particle (*i.e.*, the force of gravity acting on the displaced fluid); (*iv*) the weight of the fluid that is pulled upward or downward in the meniscus; and (*v*) the "Cheerios" forces between the free-floating particles and the target particle. (In our experiments, the target sphere never came into contact with the free particles so there were no contact forces.) The second term, the Laplace pressure, was removed from consideration by keeping the pressure reservoir in contact with our system; in this way, the Laplace pressure at a given displacement is fixed irrespective of the shape of the interface. The third and fourth terms both depend on the difference of densities of the two fluids ($\Delta\rho$) and the data in Fig. 3 show that the peak force is reduced even when ($\Delta\rho$) is smaller by 25× or 100×. The fifth term arises from the known fact that a free particle that creates a downward-sloped meniscus will attract (repel) a particle that a downward- (upward-) sloped meniscus; this is the pair-wise "Cheerios" force that pulls floating objects together [30,31]. We showed in Fig. 3 that the peak force is reduced whether the free particles pull the interface downward, upward or not at all; hence the pairwise capillary ("Cheerios") forces between the free particles and the target particle cannot explain our data and we rule out (*v*) as the principal cause.

This leaves us with the first term, the capillary force arising from the fluid interface pulling at the contact ring on the target sphere. We point out that our setup ensures that the target particle touches only clean water-air or oil-water interface, so that the force per unit length acting on the contact ring (the interfacial tension) is the pure-fluid value in all cases. Hence the free-floating particles can only reduce the peak force *via* the shape of the fluid interface where it contacts the target sphere.

In previous experiments using PDMS-coated glass spheres, we found that the receding contact angle (θ_R) varies with the shape of the interface [32]. Specifically, we found that θ_R decreased by approx. 10° when the deviatoric curvature, D, of the interface increased from 0 to 0.1 mm^{-1}. (D is a measure of shape anisotropy, defined as half the difference between the two principal curvatures.) The advancing contact angle remained unchanged. In the present experiment, the free-floating particles perturb the planar interface so that D is non-zero, though still much smaller than 0.1 mm^{-1}. In any case, calculations show that a smaller θ_R would increase F, which contradicts our data. We conclude that the force reduction cannot be attributed to a change of receding or advancing contact angle.

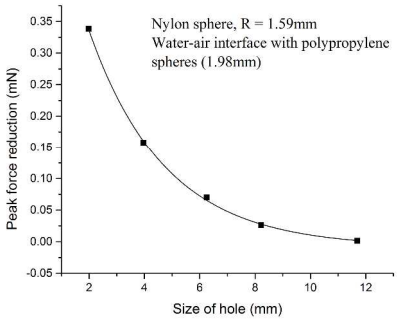

Fig. 4 Plot of the measured reduction of the peak force as a function of the hole size in the array of free-floating spheres. The solid curve shows the best fit to an exponential with a decay length of 2.8 mm.

In the above experiments, the free-floating spheres obscured the interface so we could not see its shape clearly from the side. To image the interface shape, therefore, we

used thin cover glass pieces (the square cover slips were cut into small irregular shape pieces) as the floating objects. Figure 5(a) shows the measured $F(d)$ for a PDMS coated glass sphere (1.59 mm in radius) at the interface between water and air. Here only the raising process is shown in the plot, because the shape of the meniscus around the target sphere could only be captured when it rose above the background. The result is similar to what is shown in Fig 2(b): the peak force dropped by 6% on crowded interface.

Fig 5(b) is the overlay of two images: a PDMS coated sphere at a water-air interface, and the same sphere with the same displacement at an interface crowded by particles. From this side-view image, we found that the shape of the fluid interface changed in the presence of free particles: the contact ring on the target sphere changed from a circle to an undulating ring. To see how the altered contact-line shape by itself would affect the force in a general case, we numerically calculated the vertical component of the capillary force acting on the target sphere with a contact line that undulates with quadrupolar symmetry (~cos(2ϕ) where ϕ is the polar angle in the plane of the interface). We assumed that the target sphere maintains a constant contact angle, which we find to be true for the clean interfaces. We found that the quadrupolar term makes the vertical force slightly larger (on the order of several μN), presumably because of the greater length. The predicted difference is too small to be detected by our measurements and, of course, it contradicts our finding that the force decreases. Hence, the undulation of contact line is not a major factor leading to the force drop.

We observed in our experiments that, at a fixed displacement, the size of the contact ring around the target sphere in the particle-laden interface is greater than that at the clean fluid-fluid interface, especially when the displacement is large (inset of Fig. 5(a)). The contact radius is defined as half the distance between left most and right most contact points in the image. To see how the capillary force is generically affected by a change in the contact-ring radius, we numerically calculated the vertical component of capillary force as a function of contact radius with fixed contact angle. The results indicate that the larger the contact radius is, the smaller the applied force is, which agrees with the measured $F(d)$. The reason for the larger contact radius on the crowded interface, however, is still not known, but we offer a simplified explanation in the next section.

As further evidence that the contact-ring size plays a role, we measured $F(d)$ on a PDMS-coated glass

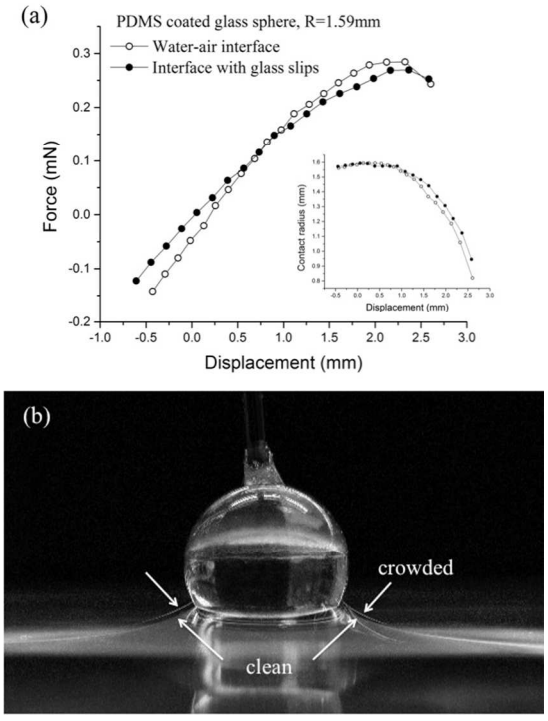

Fig. 5 (a) Measured force vs. displacement for a PDMS coated glass sphere at a water-air interface. Only the data for the raising process is shown. The inset is the corresponding contact radius as a function of displacement. (b) Overlay of an image of the PDMS-coated sphere at a clean interface (visible in the image) and at an interface crowded by particles (white curve).

cylinder oriented perpendicular to the interface. As the cylinder was pulled upward, F increased slightly because of the decreased buoyant force. Adding free-floating particles to this interface had no measurable effect on the measured force.

A simple theoretical model

The above data analysis indicates that the contact-line constraints around the free-floating particles change the shape of the interface near the target sphere, and thereby reduce the capillary force. A simplified model allows us to predict the force-displacement curve and show how this mechanism can work. We model the free spheres that are closest to the target as a toroidal ring of radius R. We then then solve the Young-Laplace equation for small interface deformation under the assumptions that the capillary length is infinite and that the contact angles on both the target sphere and toroid are constant ($\pi/2$). From the solution, we compute the displacement d of the target sphere, the contact-line radius r_c, and the force f. We find that if the target is held at a fixed d, then as the free spheres are brought closer (R is decreased), r_c increases and f decreases. Although this model does not correctly account for the deformation around the free spheres or glass pieces in our experiments, this simple model indicates that the contact-line constraints coming from free particles can perturb the interface shape so as to reduce the capillary force.

Conclusion

In summary, we have experimentally proved that the presence of floating particles at an interface can reduce the peak force needed to remove the target sphere. The results were obtained using PDMS-coated glass spheres, which have uniform and smooth contacts, and also for PTFE and nylon spheres, where the contact rings are irregular but still have well-defined contact angles. We found that the peak force was consistently reduced whether the capillary charge of free-floating particles was positive, negative or zero, and when the difference in fluid mass densities ranged from 1.0 to 0.01 g/mL. From these experiments, we ruled out gravity or buoyancy as the origin and instead concluded that the free-floating particles perturb the shape of the interface. This conclusion is supported by the images showing that the interface shape (especially the contact-ring size) are altered by the free-floating particles and also by our finding that the change in peak force decays as $\exp(-a_H/l_C)$ where a_H is the distance between the free particles and the target particle and l_C is the capillary length (Fig. 4). The force acting on a solid cylinder perpendicular to the interface was unaffected by the free-floating particles, consistent with the geometric fact that the cylinder has constant contact-line radius.

Not only does the peak force decrease, but the integrated work of removing the particle also changes. When a particle is ejected or removed from the interface by an external force, the work goes into changing the areas of the particle-fluid interfaces and of the fluid-fluid interface. (We neglect hydrodynamic dissipation because our forces are measured with stationary objects.) Once the particle snaps free of the interface, the energy stored in the excess fluid-fluid interface may be quickly dissipated as heat. Hence the work to remove a particle is larger than the binding energy. The total work to remove a PDMS coated glass sphere from the water-air interface, with its gravitational component ignored (obtained by a discrete integration of the measured $F(d)$ of Fig. 5(a))

is 4.5×10^{-7} J, which is more than twice the predicted binding energy of 1.7×10^{-7} J [2,3]. The integrated work to move a particle to the phase with lower contact angle at a particle-laden interface could be either larger (upper trace in Fig 2(b)) or smaller (Fig 5(a)) than the work at a clean interface. However, the work needed to push a particle into the phase with higher contact angle always decreases in the presence of free particles.

Although the experiments were performed on millimeter-scale particles, the fact that the results depend on interface shape and tension rather than gravity means that our results extend to micron- or nanometer-sized particles. In the latter cases, gravity and buoyancy are negligible and capillary effects predominate. In that limit, the peak force scales with interfacial tension and particle size. For the same relative particle sizes and inter-particle spacings, however, the relative change of peak force may be the same as reported here.

These results indicate that the stability of particle-laden droplets (as measured by the peak force or the work needed to remove a particle) is less than expected from single-particle measurements or theory. We attribute this effect to the fact that every free-floating particle introduces a constraint on the interface shape, and this network of constraints alters the interface shape (as shown in our experiments). These results demonstrate the need for a theory that describes effective interfacial tension or elasticity of a fluid interface crowded with particles.

Acknowledgments

This research was made possible in part by a grant from BP/The Gulf of Mexico Research Initiative through the C-MEDS consortium, and in part by the National Science Foundation (CBET-0967620 and CBET- 1438425).

References

[1] S. U. Pickering, "Emulsions," *J. Chem. Soc.* **91**, 2001 (1907).

[2] A. F. Koretsky and P. M. I. Kruglyakov, "Emulsifying Effects of Solid Particles and the Energetics of Putting them at the Water-Oil Interface," *Izv. Sib. Otd. Akad. Nauk. SSSR Ser. Khim. Nauk.* **2**, 139 (1971).

[3] P. Pieranski, "Two-Dimensional Interfacial Colloidal Crystals," *Phys. Rev. Lett.* **45**, 569 (1980).

[4] Y. Lin, H. Skaff, T. S. Emrick, A. D. Dinsmore, and T. P. Russell, "Nanoparticle Assembly and Transport at Liquid-Liquid Interfaces," *Science* **299**, 226 (2003).

[5] A. D. Dinsmore, M. F. Hsu, M. G. Nikolaides, M. Marquez, A. R. Bausch, and D. A. Weitz, "Colloidosomes: Self-Assembled, Selectively-Permeable Capsules Composed of Colloidal Particles," *Science* **298**, 1006 (2002).

[6] J. Sun and X. L. Zheng, "A review of oil-suspended particulate matter aggregation-a natural process of cleansing spilled oil in the aquatic environment," *J. Env. Monitoring* **11**, 1801 (2009).

[7] H. Katepalli, V. T. John, and A. Bose, "The Response of Carbon Black Stabilized Oil-in-Water Emulsions to the Addition of Surfactant Solutions," *Langmuir* **29**, 6790 (2013).

[8] A. Saha, A. Nikova, P. Venkataraman, V. T. John, and A. Bose, "Oil Emulsification Using Surface-Tunable Carbon Black Particles," *ACS Appl. Mater. Interfaces* **5**, 3094 (2013).
[9] R. Aveyard, B. P. Binks, and J. H. Clint, "Emulsions stabilised solely by colloidal particles," *Adv. Coll. Int. Sci.* **100**, 503 (2003).
[10] P. Chaudhuri, S. Karmakar, C. Dasgupta, H. R. Krishnamurthy, and A. K. Sood, "Equilibrium glassy phase in a polydisperse hard-sphere system," *Phys. Rev. Lett.* **95**, 248301 (2005).
[11] B. Madivala, S. Vandebril, J. Fransaer, and J. Vermant, "Exploiting particle shape in solid stabilized emulsions," *Soft Matter* **5**, 1717 (2009).
[12] A. Stocco, E. Rio, B. P. Binks, and D. Langevin, "Aqueous foams stabilized solely by particles," *Soft Matter* **7**, 1260 (2011).
[13] N. Chatterjee and M. Flury, "Effect of Particle Shape on Capillary Forces Acting on Particles at the Air-Water Interface," *Langmuir* **29**, 7903 (2013).
[14] N. Chatterjee, S. Lapin, and M. Flury, "Capillary Forces between Sediment Particles and an Air-Water Interface," *Environ. Sci. Technol.* **46**, 4411 (2012).
[15] O. Pitois and X. Chateau, "Small particle at a fluid interface: Effect of contact angle hysteresis on force and work of detachment," *Langmuir* **18**, 9751 (2002).
[16] G. D. Yarnold, "The Hysteresis of the Angle of Contact of Mercury," *Proc. Phys. Soc. London* **58**, 120 (1946).
[17] A. D. Scheludko and A. D. Nikolov, "Measurement of Surface-Tension by Pulling a Sphere from a Liquid," *Colloid Polym. Sci.* **253**, 396 (1975).
[18] C. Huh and S. G. Mason, "Sphere Tensiometry - Evaluation and Critique," *Canadian Journal of Chemistry-Revue Canadienne De Chimie* **54**, 969 (1976).
[19] L. Zhang, L. Ren, and S. Hartland, "More convenient and suitable methods for sphere tensiometry," *J. Colloid Interface Sci.* **180**, 493 (1996).
[20] L. Zhang, L. Ren, and S. Hartland, "Detailed analysis of determination of contact angle using sphere tensiometry," *J. Colloid Interface Sci.* **192**, 306 (1997).
[21] P.-G. de Gennes, F. Brochard-Wyart, and D. Quéré, *Capillarity and Wetting Phenomena: Drops, Bubbles, Pearls, Waves* Springer, New York, NY, 2004.
[22] M. Preuss and H. J. Butt, "Measuring the contact angle of individual colloidal particles," *J. Colloid Interface Sci.* **208**, 468 (1998).
[23] G. Gillies, M. Kappl, and H. J. Butt, "Direct measurements of particle-bubble interactions," *Adv. Colloid Interface Sci.* **114**, 165 (2005).
[24] J. W. Krumpfer and T. J. McCarthy, "Contact angle hysteresis: a different view and a trivial recipe for low hysteresis hydrophobic surfaces," *Faraday Discuss.* **146**, 103 (2010).
[25] P. A. Kralchevsky and K. Nagayama, "Capillary interactions between particles bound to interfaces, liquid films and biomembranes," *Adv. Colloid Interface Sci.* **85**, 145 (2000).
[26] D. Stamou, C. Duschl, and D. Johannsmann, "Long-range attraction between colloidal spheres at the air- water interface: The consequence of an irregular meniscus," *Phys. Rev. E* **62**, 5263 (2000).
[27] A. Dominguez, D. Frydel, and M. Oettel, "Multipole expansion of the electrostatic interaction between charged colloids at interfaces," *Phys. Rev. E* **77**, 020401 (2008).

[28] W. S. Rasband, (U. S. National Institutes of Health, Bethesda, Maryland, USA, 1997-2011).
[29] M. M. Nicolson, "The Interaction between Floating Particles," *Proceedings of the Cambridge Philosophical Society* **45**, 288 (1949).
[30] D. Vella and L. Mahadevan, "The "Cheerios effect"," *Am. J. Phys.* **73**, 817 (2005).
[31] M. M. Nicolson, "The Interaction between Floating Particles," *Proc. Cambridge Phil. Soc.* **45**, 288 (1949).
[32] N. Senbil, W. He, V. Démery, and A. D. Dinsmore, "Effect of Interface Shape on Advancing and Receding Fluid-Contact Angles around Spherical Particles," *(submitted for publication)* (2014).